

## Article

# Bio-Composite Filaments Based on Poly(Lactic Acid) and Cocoa Bean Shell Waste for Fused Filament Fabrication (FFF): Production, Characterization and 3D Printing

Daniela Fico <sup>1,2</sup>, Daniela Rizzo <sup>3,\*</sup>, Valentina De Carolis <sup>1</sup> and Carola Esposito Corcione <sup>1</sup>

<sup>1</sup> Department of Engineering for Innovation, University of Salento, Edificio P, Campus Ecotekne, s.p. 6 Lecce-Monteroni, 73100 Lecce, Italy; daniela.fico@unisalento.it (D.F.); valentina.decarolis@unisalento.it (V.D.C.); carola.corcione@unisalento.it (C.E.C.)

<sup>2</sup> Italian National Council of Research-Institute of Heritage Sciences (CNR-ISPC), Campus Ecotekne, 73100 Lecce, Italy

<sup>3</sup> Department of Cultural Heritage, University of Salento, Via D. Birago 64, 73100 Lecce, Italy

\* Correspondence: daniela.rizzo@unisalento.it

**Abstract:** In this study, novel biocomposite filaments incorporating cocoa bean shell waste (CBSW) and poly(lactic acid) (PLA) were formulated for application in Fused Filament Fabrication (FFF) technology. CBSW, obtained from discarded chocolate processing remnants, was blended with PLA at concentrations of 5 and 10 wt.% to address the challenge of waste material disposal while offering eco-friendly composite biofilaments for FFF, thereby promoting resource conservation and supporting circular economy initiatives. A comprehensive analysis encompassing structural, morphological, thermal, and mechanical assessments of both raw materials and resultant products (filaments and 3D printed bars) was conducted. The findings reveal the presence of filler aggregates only in high concentrations of CBSW. However, no significant morphological or thermal changes were observed at either CBSW concentration (5 wt.% and 10 wt.%) and satisfactory printability was achieved. In addition, tensile tests on the 3D printed objects showed improved stiffness and load resistance in these samples at the highest CBSW concentrations. In addition, to demonstrate their practical application, several 3D prototypes (chocolate-shaped objects) were printed for presentation in the company's shop window as a chocolate alternative; while retaining the sensory properties of the original cocoa, the mechanical properties were improved compared to the base raw material. Future research will focus on evaluating indicators relevant to the preservation of the biocomposite's sensory properties and longevity.

**Keywords:** waste; cocoa shell; 3D printing; fused filament fabrication; PLA; circular economy



**Citation:** Fico, D.; Rizzo, D.; De Carolis, V.; Esposito Corcione, C. Bio-Composite Filaments Based on Poly(Lactic Acid) and Cocoa Bean Shell Waste for Fused Filament Fabrication (FFF): Production, Characterization and 3D Printing. *Materials* **2024**, *17*, 1260. <https://doi.org/10.3390/ma17061260>

Academic Editor: Young-Hag Koh

Received: 31 January 2024

Revised: 28 February 2024

Accepted: 6 March 2024

Published: 8 March 2024



**Copyright:** © 2024 by the authors. Licensee MDPI, Basel, Switzerland. This article is an open access article distributed under the terms and conditions of the Creative Commons Attribution (CC BY) license (<https://creativecommons.org/licenses/by/4.0/>).

## 1. Introduction

Respect for the environment and sustainability are issues of great concern today due to the growing problem of the disposal of industrial production waste. The circular economy (CE), a sustainable system that aims to reduce the consumption of raw materials and the production of waste by reintegrating them into a closed production cycle, underpins this research effort [1,2]. Disposal poses a significant challenge in the food industry, exacerbated by factors such as population growth. In particular, the escalating global demand for chocolate, a popular foodstuff in confectionery around the world, has led to a dramatic increase in the production of cocoa bean shell waste (CBSW) [3]. CBSW (100% cocoa bean shell) is typically repurposed as organic fertilizer, animal feed, or fuel, albeit with adverse environmental consequences [4]. In very few studies, CBSW is used as a renewable resource and as an additive to polymer matrix such as poly(lactic acid), PLA, which is known for its versatility and suitability in 3D printing with FFF technology [5,6]. Among the various methods for recycling waste materials, additive manufacturing (AM), or 3D printing, which

facilitates the production of complex prototypes from computer-aided design (CAD) models while minimizing material waste [7,8], may be one of the most promising techniques. Its versatility extends to various industries, including advanced medicine and food processing, aligning with the transition from a linear to a circular economy model [9–11]. Previous research has demonstrated AM's potential to reduce waste production, enhance product value, and promote sustainability [12–14]. Studies by Sanyang et al. [15], Papadopoulou et al. [16], and Tran et al. [17] have explored the use of cocoa waste in composite films and biocomposites, showcasing its potential as a natural filler with ecological benefits. Additionally, Leonard and Berrio [18] investigated PLA-based filaments incorporating cocoa husk for biomedical applications, noting improvements in compressive strength without altering thermal properties [19,20]. Andres J. Garcia-Brand et al. [21] pioneered a method for utilizing CBSW as reinforcement to enhance the bioactivity of synthetic polymeric materials in biomedical research. TGA and DSC thermograms unveiled the feasibility of employing various processing techniques, such as compression molding, extrusion, and potentially 3D printing. However, they did not explore the utilization of any 3D printing technology for fabricating 3D models using composite materials. In this study, biofilaments comprising PLA and CBSW at varying concentrations were developed and used to produce 3D models by FFF, offering a novel approach to waste recycling and reuse through FFF printing. The findings highlight the feasibility of integrating waste materials into the production cycle while emphasizing the importance of sustainable practices in modern manufacturing [22–25]. Based on this scenario, the aim of this study was to develop and characterize biocomposite filaments made from poly(lactic acid) and 5–10 wt.% of cocoa bean shell waste for FFF printing technology, from a CE perspective. The developed green filaments were subjected to morphological–structural, thermal and mechanical analyses. For the first time, the authors tested the feasibility of the FFF printing process to produce new 3D objects from waste materials, with the aim of permitting their integration into the same material production cycle (company-to-company). The work highlights the importance of sustainable practices in modern manufacturing while using solvent-free, inexpensive and easy-to-use methods.

## 2. Materials and Methods

The technical specifications of the materials utilized for the creation of composite biofilaments, manufacturing methodologies, and analytical techniques for structural, morphological, thermal, and mechanical characterization are outlined as follows.

### 2.1. Materials

The Ingeo 4043D poly(lactic acid) (NatureWorks LLC, Blair, NE, USA) employed as the polymer matrix for fabricating the composite filaments was obtained in pellet form. It possesses a density of  $1.24 \text{ g cm}^{-3}$  and a melt flow index (MFI) of  $6 \text{ g}/10 \text{ min}$  at a temperature of  $210 \text{ }^\circ\text{C}$ . PLA was utilized both independently to produce a virgin filament (100PLA) and as a polymer matrix for creating two biofilaments incorporating CBSW as fillers at 5 wt.% and 10 wt.%, respectively. Initially, the PLA pellets, with a diameter of approximately 5 mm (manufacturer's data sheet), were stored in an oven at  $60 \text{ }^\circ\text{C}$  for 24 h before being reduced into particles using the Retsch ZM 100 Ultracentrifugal mill (Retsch GmbH, Haan, Germany) equipped with a sieve with a mesh diameter of 0.75 mm.

The cocoa bean shell waste (CBSW) utilized in the production of the new composite filaments originates from the manufacturing residues of the company "Maglio Arte Dolciaria S.R.L." (Maglie, Lecce, Apulia, Italy). Supplied by the company in the form of coarse-grained and heterogeneous powder, it exhibits the characteristic brown color of cocoa and a robust chocolate-like odor. Prior to utilization, the CBSW was subjected to storage in an oven at  $60 \text{ }^\circ\text{C}$  for 24 h and subsequently reduced into particles using the Retsch ZM 100 Ultracentrifugal mill (Retsch GmbH, Haan, Germany) equipped with a sieve with a mesh diameter of 0.25 mm.

## 2.2. Production of Biofilaments for FFF

The PLA and CBSW powders were initially combined manually at room temperature before being introduced into the extrusion chamber of the 3Devo Composer 450 Filament Maker single-screw extruder (Utrecht, The Netherlands), as reported in Figure 1.

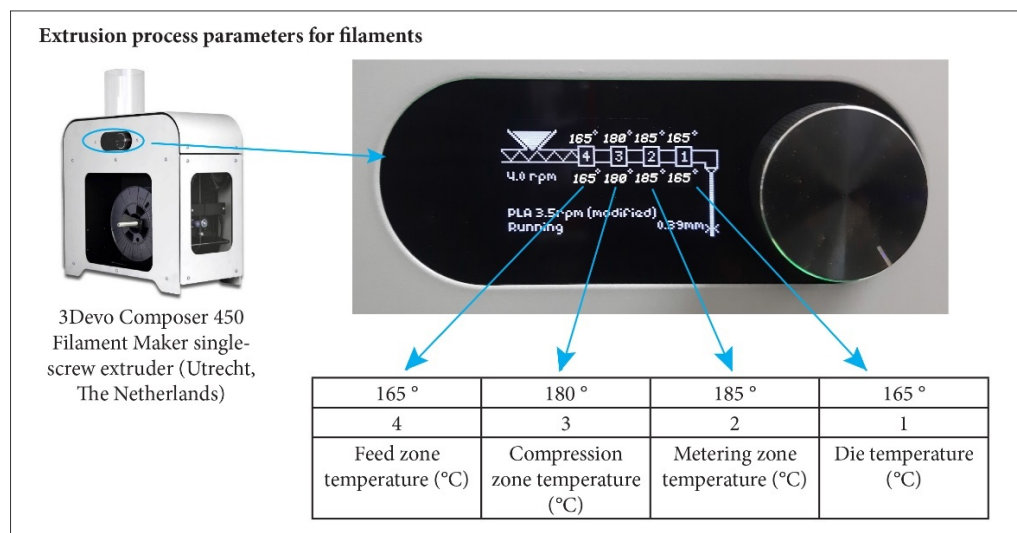


**Figure 1.** 3Devo Composer 450 Filament Maker single-screw extruder with indication of different temperature zones.

The parameters used to produce the filaments by the extrusion process are outlined in Table 1, while the labels and compositions of the materials used and developed are listed in Table 2.

**Table 1.** Extrusion process parameters for filaments.

Extrusion Process Parameters	100PLA	95PLA/5CBSW	90PLA/10CBSW
Screw speed (rpm)	3.5	4	4
Fan cooling speed (%)	0	30	30
Feed zone temperature (°C)	170	165	165
Compression zone temperature (°C)	185	180	180
Metering zone temperature (°C)	190	185	185
Die temperature (°C)	200	165	165

**Table 2.** Raw Materials, biofilament and 3D printed sample labels and weight composition (wt.%).

Label	Type	Composition (wt.%)
PLA	Raw material	100 PLA Ingeo 4043D pellet
CBSW	Raw material	100 Cocoa bean shell waste powder
100PLA	Filament	100 PLA Ingeo 4043D
95PLA/5CBSW	Filament	95 PLA Ingeo 4043D and 5 Cocoa bean shell waste
90PLA/10CBSW	Filament	90 PLA Ingeo 4043D and 10 Cocoa bean shell waste
100PLA_3D	3D sample	100 PLA Ingeo 4043D
95PLA/5CBSW_3D	3D sample	95 PLA Ingeo 4043D and 5 Cocoa bean shell waste
90PLA/10CBSW_3D	3D sample	90 PLA Ingeo 4043D and 10 Cocoa bean shell waste

## 2.3. 3D Printing

Three-dimensional samples were printed on the Creality CP-01 printer (Creality, London, UK) in accordance with the European standard used for the tensile tests ISO 527-2(2012) [26]. The following printing parameters were used: extrusion temperature 200 °C, plate temperature 50 °C, print speed 50 mm/s, fill 100% and fan speed 100%.

The CAD model was developed using Fusion 360 software (Autodesk, San Rafael, CA, USA) and converted to a G-code file using Cura software, Ultimaker Cura version 5.1.1. (Ultimaker B.V., Utrecht, The Netherlands). Finally, after studying the structural, thermal and mechanical properties of the biocomposites, some design objects (some traditional chocolate shapes) were printed for display in the window of the company that supplied the cocoa waste. The CAD models were developed using Fusion 360 software (Autodesk, San Rafael, CA, USA) and converted to Gcode files using Cura software, (Ultimaker B.V., Utrecht, The Netherlands). Prints were made with the Creality CP-01 printer (Creality, London, UK) with the following operating parameters: extrusion temperature 190 °C, plate temperature 50 °C, print speed 60 mm/s and infill 20%.

Three-dimensional objects (chocolate shaped objects) were also printed to demonstrate the printability of complex shapes with the recycled filaments. For this purpose, the BQ Hephestos 2 printer (BQ, Barcelona, España) was used with the following printing parameters: extrusion temperature 200 °C, plate temperature 0 °C, printing speed 60 mm/s and infill 20%.

A comprehensive list of all materials employed in this study is provided in Table 2.

#### 2.4. Methods

The morphological characterization of the raw materials and the biofilaments produced was carried out using a scanning electron microscope (SEM), model Zeiss E Evo 40 (Oberkochen, Germany).

Fourier transform infrared spectroscopy (FTIR) analyses were performed on the raw materials (PLA and CBSW powders) to perform a preliminary chemical structural characterization. FTIR spectra were obtained on KBr pellets using a JASCO FT/IR 6300 spectrometer (Easton, MD) with a resolution of 4 cm<sup>-1</sup>, setting up 64 scans in the region between 4000 and 600 cm<sup>-1</sup>. Five spectra were considered for each replicate sample.

XRD measurements of the raw materials and biofilaments were performed with a Rigaku Ultima + diffractometer (Tokyo, Japan) using CuK $\alpha$  radiation ( $\lambda = 1.5418 \text{ \AA}$ ) in the step scan mode, recorded in the  $2\theta$  range from 2–60°, with a step size of 0.02° and a step duration of 0.5 s. Five spectra were considered for each replicate sample.

DSC analysis (Mettler Toledo DSC1 StareSystem) was performed on raw materials, filaments and 3D printed rods to investigate thermal properties by measuring the glass transition temperature ( $T_g$ ), crystallization temperature ( $T_c$ ) and melting temperature ( $T_m$ ). The analyses were performed over a temperature range of 25 °C to 200 °C at a heating rate of 10 °C/min.

According to the ISO 527-2(2012) standard [26], tensile tests were performed on the 3D printed sample using a Lloyd LR5K dynamometer (Lloyd Instruments Ltd., Bognor Regis, UK) at a strain rate of 1 mm/min. The grips used in these tests were wedge-type grips, the distance between grips was 58 mm, and the load cell was 5 kN. The dimensions of the specimen refer to the 1BA type, according to the standard. Five replicates were performed for each specimen.

Magnified images of the sections of the 3D printed tensile samples were obtained using the Dino Lite digital microscope instrument (AnMo Electronics Corporation, New Taipei City, Taiwan) to understand the morphology and adhesion of the different deposited layers.

### 3. Results and Discussion

#### 3.1. Characterization of Raw Materials

The morphological–structural, chemical and thermal features of all raw materials used to produce biofilaments were investigated. The results of the SEM, FTIR, XRD and DSC analyses of the raw materials are shown below.

After the milling process, SEM images (Figure 2A,B) at high magnifications (100 $\times$  and 1000 $\times$ ) of the neat PLA particles show an irregular, square shape and a diameter up to about 500  $\mu\text{m}$ . The cocoa bean shell waste (CBSW) was supplied in the form of a

coarse-grained, inconstant powder, after grinding the cocoa bean shell. Furthermore, as visible from the SEM image (Figure 2C,D), the CBSW particle size varies from about 5  $\mu\text{m}$  to about 200  $\mu\text{m}$ .

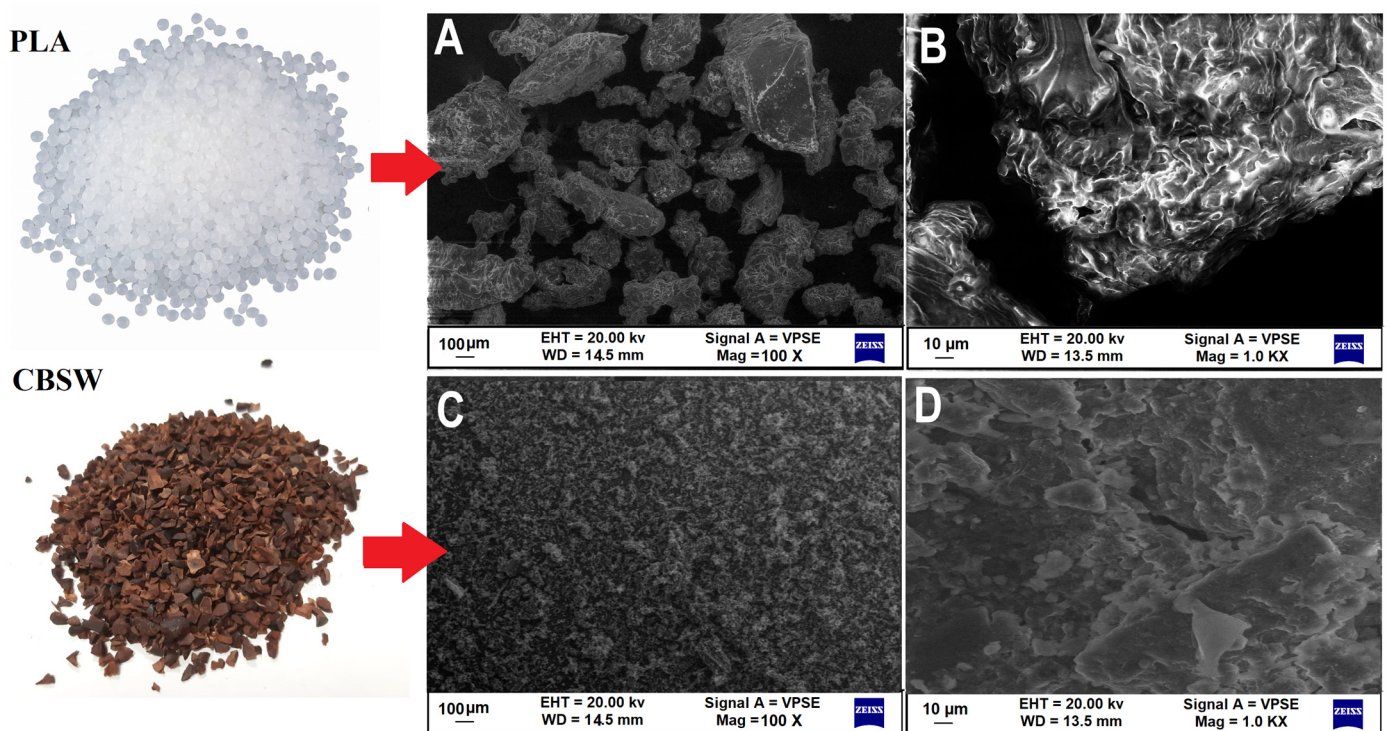


**Figure 2.** SEM images of raw materials: (A) PLA pellet magnification 100 $\times$  and (B) magnification 1K $\times$ ; (C) cocoa bean shell waste magnification 100 $\times$  and (D) magnification 1K $\times$ .

The chemical characterization of the raw materials was carried out using FTIR spectroscopy. The infrared spectra of PLA powder and CBSW are shown in Figure 3.

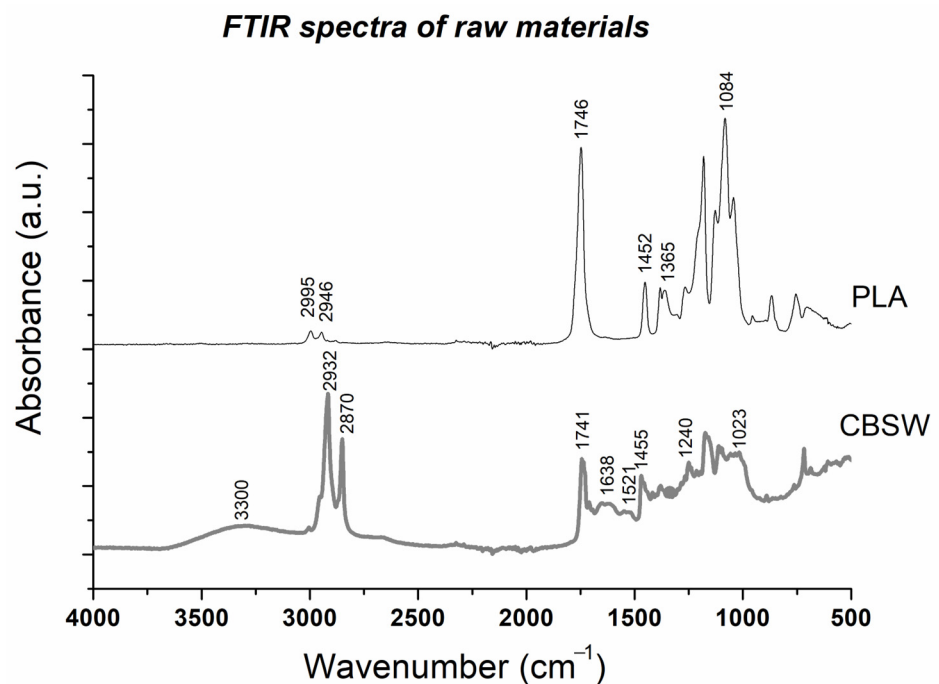


**Figure 3.** FTIR spectra of PLA pellet and cocoa bean shell waste and main infrared peaks.

The infrared spectrum of the PLA shows asymmetrical and symmetrical  $-\text{CH}_3$  and  $-\text{CH}_2$  stretching frequencies at  $2995\text{ cm}^{-1}$  and  $2946\text{ cm}^{-1}$ , respectively, and a characteristic peak of  $\text{C}=\text{O}$  stretching at about  $1746\text{ cm}^{-1}$  [27]. The peaks at  $1452\text{ cm}^{-1}$  and  $1365\text{ cm}^{-1}$  are associated with the asymmetric and symmetric bending vibrations of the  $-\text{CH}_3$  groups, respectively, while the band at about  $1084\text{ cm}^{-1}$  corresponds to the  $\text{C}-\text{O}$  bond [27].

In the FTIR spectrum of the CBSW, the band present at around  $3300\text{ cm}^{-1}$  is associated with OH groups, while the peaks at  $2932\text{ cm}^{-1}$  and  $2870\text{ cm}^{-1}$  correspond to the asymmetric and symmetric stretching vibrations of the  $\text{C}-\text{H}$  groups of cellulose and hemicellulose. The infrared peak at  $1741\text{ cm}^{-1}$  corresponds to the  $\text{C}=\text{O}$  stretching of saturated esters, while the three infrared bands at approximately  $1638\text{ cm}^{-1}$ ,  $1521\text{ cm}^{-1}$  and  $1401\text{ cm}^{-1}$  correspond to amide I, II and III, respectively. These bands can be associated with proteins, lignin and polysaccharides present in the biomass. Finally, the peaks at  $1240\text{ cm}^{-1}$  and  $1023\text{ cm}^{-1}$  are associated with holocellulose biomolecules [28].

In the XRD diffractogram of the PLA (Figure 4A), more defined diffraction peaks emerge at  $2\theta = 16.70^\circ$  and at  $2\theta = 19.10^\circ$  over a broad amorphous band, assigned to the crystalline plane (110) and (203), respectively [14]. The diffractogram of the CBSW sample (Figure 4A) shows peaks at  $2\theta = 3.09^\circ$ ,  $19.5^\circ$ ,  $21.20^\circ$ ,  $22.02^\circ$  (002),  $23.11^\circ$  and  $24.30^\circ$ , some of which are characteristic of crystalline polymorphs of cellulose [29,30]. The cocoa bean from which the powder was obtained is composed of about 60 wt.% water and holocellulose (cellulose, hemicellulose, pectin) and then lignin [29] and its XRD diffractogram is very similar to cocoa butter [31].

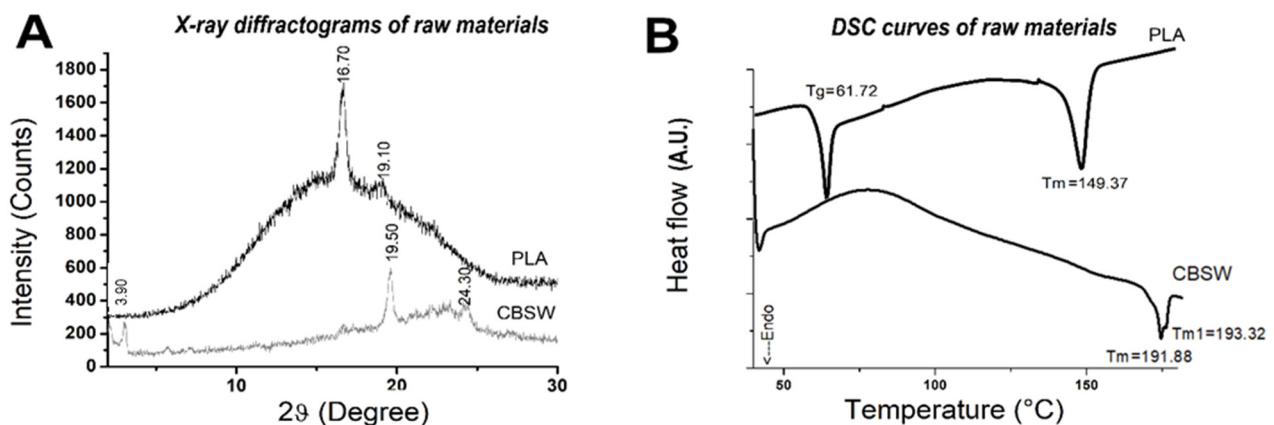


**Figure 4.** (A) XRD diffractograms and (B) DSC curve of raw materials.

A DSC analysis was performed on raw materials to investigate thermal properties (Figure 4B). In the DSC curve of poly(lactic acid), the glass transition temperature ( $T_g$ ) was measured using the inflection point method with the STARe System version 11 software (Mettler Toledo, Milan, Italy) [12] and corresponds for PLA to  $61.72^\circ\text{C}$ . In Figure 4B, it is also observed that the  $T_g$  is accompanied by an endothermic peak (relaxation enthalpy) due to the transformation of the polymer from the glassy to the liquid-viscous or rubbery state [32]. The DSC curve also shows a melting peak at temperature  $T_m$  of  $149.37^\circ\text{C}$  and melting enthalpy  $\Delta H_m$  of  $19.90\text{ J/g}$ . In the present investigation, the DSC curves of CBSW samples were also examined. As with PLA, the average values obtained from the five measurements are shown in Figure 4B. The DSC analysis was carried out in the maximum temperature range commonly used in FFF printing with PLA filaments, i.e., between  $25$  and  $200^\circ\text{C}$ . CBSW is a complex biomass consisting of several components, such as proteins, lignin and polysaccharides, as previously reported. Moreover, similar to woody biomass, the main polysaccharide components, consisting of hemicellulose, cellulose and lignin, manifest maximum endothermal peaks in different ranges according to the scientific literature [33,34]. Therefore, it can be concluded that the double endothermic peak present

in the CBSW-DSC curve only refers to the thermal decomposition of hemicellulose and partially of cellulose.

### 3.2. Characterization of Biofilaments

SEM analyses were performed on the external surfaces of the composite filaments to investigate surface roughness and on the cross-section of filaments to verify homogeneity (Figure 5). The surface of the composite filament becomes slightly irregular after the addition of CBSW (Figure 5D–F), and some discontinuity areas are observed (Sample 95PLA/5CBSW). This phenomenon becomes more pronounced with the increase in the amount of filler added to the polymer matrix (Sample 90PLA/10CBSW), where the surface appears completely rough (Figure 5G–I). Furthermore, as shown by the cross-sectional images of the two produced FFF biofilaments, the cocoa particles aggregate in some places and these aggregates are even more visible in the filament containing 10 wt.% CBSW. The phenomenon appears to be attributable not only to a different diameter of the particles in the mixture (PLA approximately 500  $\mu\text{m}$  measured by SEM and CBSW 5  $\mu\text{m}$  to 1 mm diameter measured by SEM), but also to a different chemical nature that creates poor interfacial adhesion. This occurrence is already known in the literature for various PLA-based composites and waste fillers with different polarities and may indicate the possibility in the future of using plasticizer agents that improve the compatibility and adhesiveness of the different substances [35].

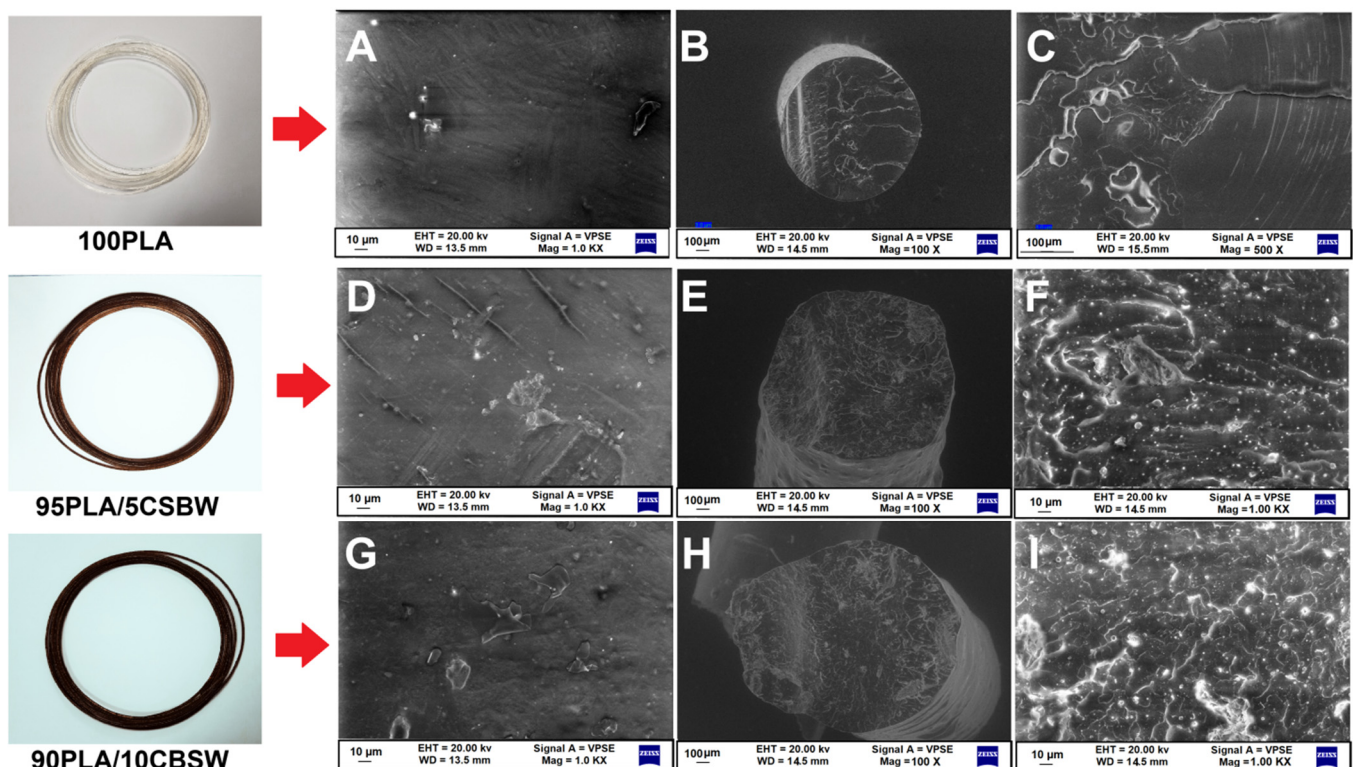


**Figure 5.** SEM images of filaments: (A) 100PLA external filament surface magnification 1.0K $\times$ , (B) section magnification 100 $\times$  (C) section magnification 500 $\times$ ; (D) 95PLA/5CBSW external filament surface magnification 1.0K $\times$ , (E) section magnification 100 $\times$ , (F) section magnification 1.0K $\times$ ; (G) 90PLA/10CBSW external filament surface magnification 1.0K $\times$ , (H) section magnification 100 $\times$ , (I) section magnification 1.0K $\times$ .

XRD spectra of filaments show only amorphous bands and a remarkable decrease in the intensity of diffraction peaks relative to the raw materials (Figure 6A). However, no major differences are shown between the 100PLA filament and the 95PLA/5CBSW and 90PLA/10CBSW filaments, indicating that the reticular parameters of the PLA crystal struc-

ture remained unchanged after coextrusion of the polymer with CBSW. Similar observations were also reported by Tran et al. 2017 for poly( $\epsilon$ -caprolactone) matrix biocomposites [17]. Therefore, to obtain information on the variation in the thermal properties of composite filaments compared to pure materials, a DSC analysis was performed (Figure 6B). The DSC thermograms of the PLA-based biofilaments or PLA and CBSW-based filaments are shown in Figure 5B. The glass temperatures ( $T_g$ ) of all materials were measured using the inflection point: the  $T_g$  coincides with the point at which the second derivative is equal to zero. The  $T_g$  measured for the 100PLA sample was 59.19 °C, a value similar to that reported in the literature [1] and slightly lower than that of the starting pellet.

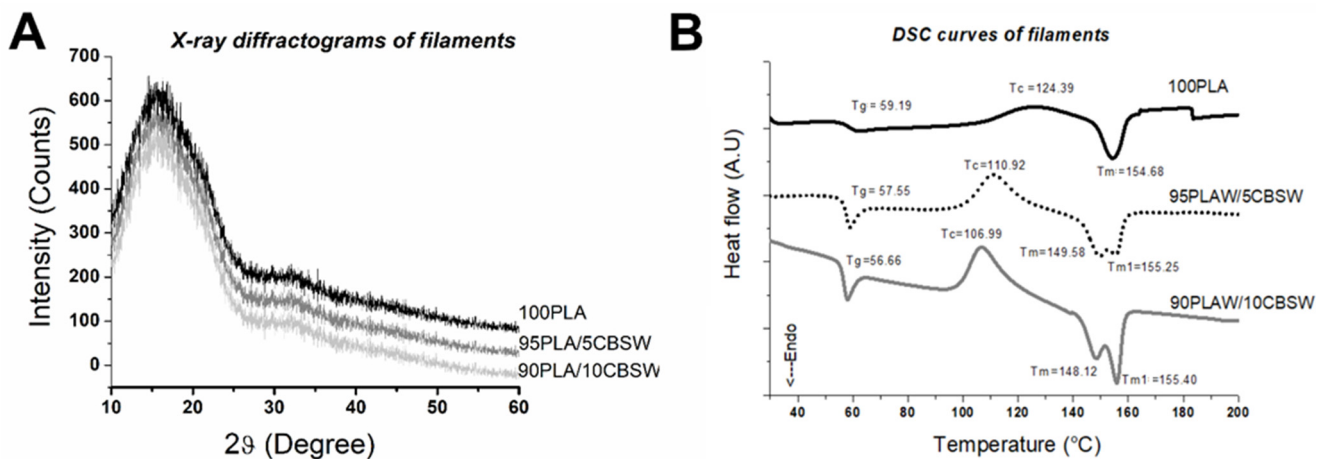


**Figure 6.** (A) XRD diffractograms and (B) DSC curves of filaments.

Composite filaments show a lower  $T_g$  than the PLA filament. This suggests that the cocoa particles interacted with the PLA on a molecular scale. However, the main differences due to this interaction process between the polymer chains and the filler are found in the crystallization ( $T_c$ ) and melting ( $T_m$ ) temperatures. The crystallization temperature  $T_c$  in the 95PLA/5CBSW and 90PLA/10CBSW filaments compared to the 100PLA filament having a  $T_c$  of 124.39 °C decreases to 110.92 °C and 106.99 °C, respectively. Furthermore, the melting process seems to be particularly influenced by the presence of the CBSW filler, which leads to the development of a double melt peak ( $T_m$  and  $T_{m1}$ ) in composite biofilaments, which is absent in 100PLA (Figure 6B). Similar behaviour and the presence of the double melting peak were observed by the authors in biocomposites based on polylactic acid and olive wood waste, indicating a different behaviour during the phase transition between the polymer and the organic filler [35].

Leonard and Berrio, on the other hand, highlighting the same characteristic in the PLA-based filaments and cocoa bean shells they have developed and which have not undergone any chemical treatment, attribute the existence of two peaks during melting to the different degradation temperatures of hemicellulose and cellulose present in the filler [18]. This last interpretation seems to be in agreement with the DSC curve of CBSW obtained in our study and shown in Figure 4B.

### 3.3. Characterization of 3D Samples

Three-dimensional specimens for tensile testing were produced by FFF printing in accordance with ISO 527-2(2012) [26]. The overall average results are shown in Figure 7. The results of the pure PLA samples are consistent with those reported in the literature [1].

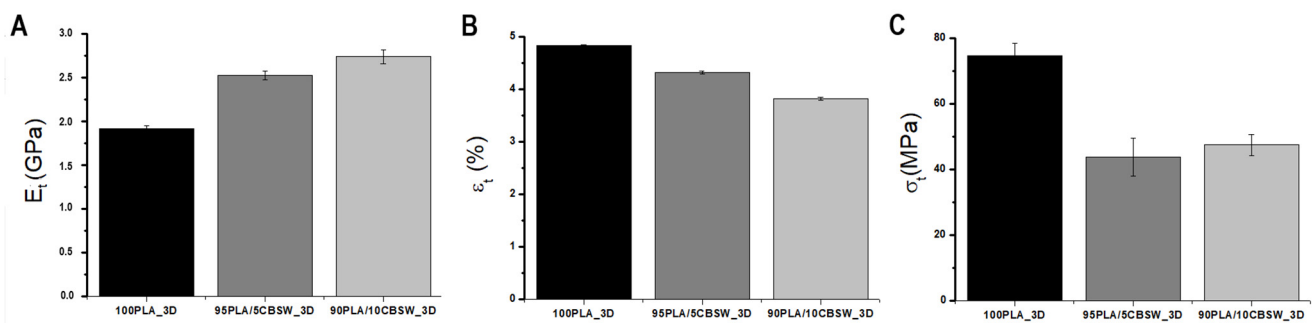


**Figure 7.** Mechanical properties from tensile tests of 3D samples: (A) Young's modulus  $E_t$  (GPa), (B) elongation at break  $\epsilon_t$  (%), (C) maximum strength (MPa).

The Young's modulus ( $E_t$ ) increased in the CBSW-based samples. Indeed, an inevitable consequence of the addition of filler to the polymer matrix is an increase in the viscosity of the polymer melt, which usually depends on the volume fraction of filler and the size and shape of the particles (Figure 7A) [36]. Overall, the presence of filler appears to have hindered the mobility of the polymer chain of the PLA matrix, thereby increasing the stiffness of the 3D sample composite. Furthermore, this increase appears to be linear, as observed by the  $E_t$  value increasing with filler wt.%. It has been reported in the scientific literature that the addition of the filler actually modifies the polymer phase and the polymer interacts with the filler surface to form an adsorbed polymer interphase [36]. The thickness of this interphase (as well as the value of the Young's modulus) depends on the bond between the polymer and the filler, which in turn depends on the surface area (i.e., the shape and size of the filler particles). Based on these considerations, the different behaviours of the composites could probably be due to a stronger interaction between the polymer and the filler in the 90PLA/10CBSW\_3D sample, caused by the larger specific active surface area of the CBSW particles, as well as the higher volume fraction of the filler [36].

The elongation at break  $\epsilon_t$  (%) always decreases with the addition of filler to pure PLA (Figure 7B), in agreement with the literature [17,30], leading to an increase in the fragility of the composites compared to the polymer. Similarly, the value of the maximum strength  $\sigma_t$  (MPa) decreases in both the 95PLA/5CBSW\_3D and 90PLA/10CBSW\_3D samples (Figure 7C) with a non-linear trend. This is probably due to a different orientation of the filler particles dispersed in the polymer matrix. Overall, the tensile test results show a lower ductility and a change in the mechanical properties of CBSW based composites; the non-uniform distribution of CBSW particles in the composite structure is the main cause.

The DSC analysis performed on the FFF printed 3D samples is shown in Figure 8. A decrease in glass transition temperature ( $T_g$ ) is observed for all 3D samples compared to the pure PLA 3D sample. The crystallization ( $T_c$ ) and melting temperatures ( $T_m$  and  $T_{m1}$ ) of the CBSW-based samples also decrease but remain higher than those measured for the corresponding composite filaments, indicating a greater interaction between the polymer chains and the filler and a higher degree of crystallinity after the printing process. This also explains the increase in Young's modulus of the CBSW-based 3D samples described above. There is also always a double melting peak in 3D samples due to the presence of the filler in the polymer matrix, i.e., different phases.

To better understand the printability of the developed biofilaments, a microscopic analysis was performed along the side surface of the 3D samples. The images obtained by light microscopy are shown in Figure 9 and overall show good adhesion between the 3D layers in both the 100PLA\_3D sample (Figure 9A) and in the 95PLA/5CBSW\_3D sample (Figure 9B), in contrast to the 90PLA/10CBSW\_3D sample (Figure 9C). The addition of CBSW filler to the polymer matrix, which causes the formation of particle aggregates in the filament, causes adhesion problems between the layers in the 90PLA/10CBSW\_3D; as in the other 3D samples, the layers are perfectly aligned with each other and do not show

swelling, deformation, or detachment; however, the presence of some air voids is observed, and this porosity probably inhibits the mechanical performance of the composite material.

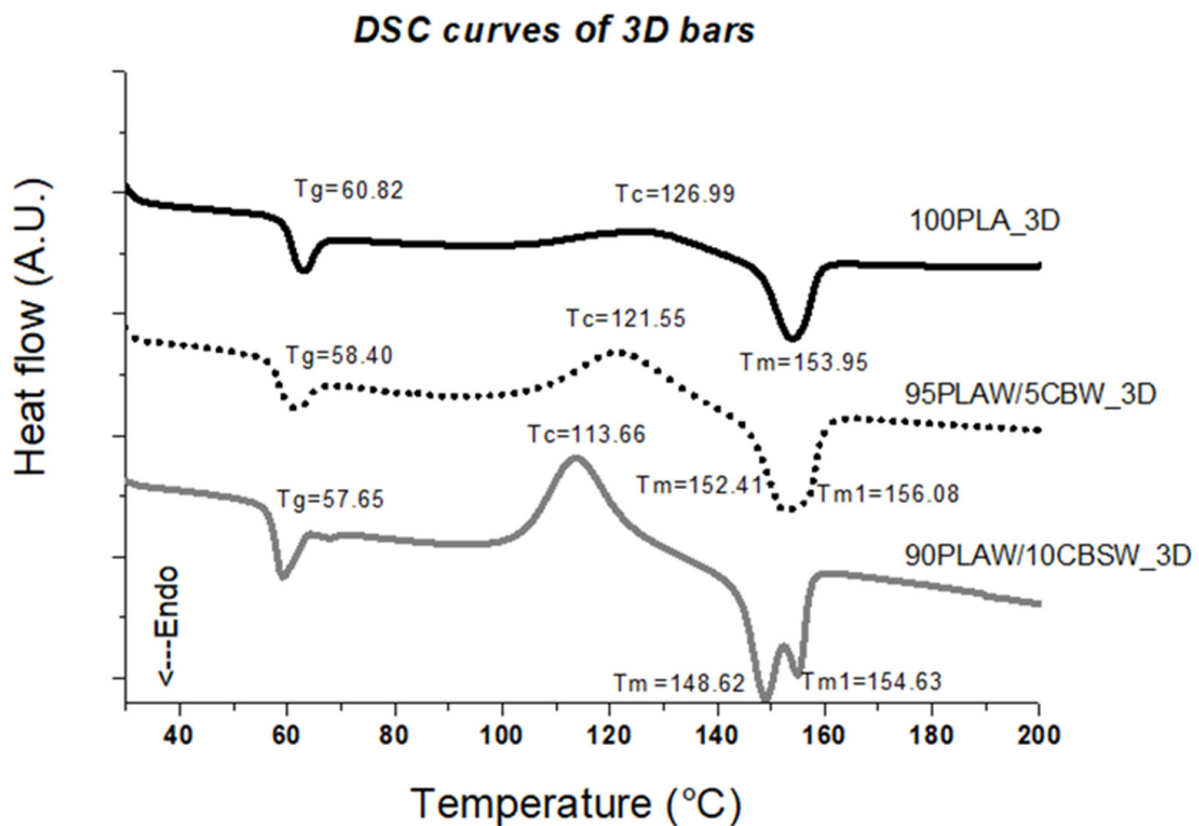


**Figure 8.** DSC curves of 3D samples.

### 3.4. From Agro-Industrial Waste to New Objects

In this work, the waste materials, i.e., cocoa bean shell waste CBSW, were supplied as a residue from the chocolate manufacturing process in the form of a coarse-grained, non-homogeneous powder. These are residues from chocolate processing that the company must necessarily discard, with a significant time and economic effort. In this section, the authors want to illustrate an example of one of the many sustainable applications that can be imagined, i.e., reusing recycled materials to create a new object that can be redeployed by the same company that produced the waste. Based on the tested performance of the developed cocoa and poly(lactic acid) biofilaments, the 90PLA/10CBSW filament was selected for 3D printing the chocolate-shaped objects (prototypes) using Fused Filament Fabrication 3D printing technology (Figure 10). Specifically, the authors chose to produce 3D printed objects in the shape of traditional chocolates or other shapes, so that they could be used by the supplier company for display in the shop window or inside the shop as design and furnishing objects, having greater durability and resistance to environmental conditions than real chocolate. The final object after printing preserves the same environmental resistance characteristics as the 3D bars tested in the previous paragraph. Most interestingly is that already the 5 wt.% of cocoa powder (CSBW) product allows the organoleptic characteristics of pure chocolate to be preserved in the 3D object, giving customers the feeling that it is a real product exhibited in a store window.

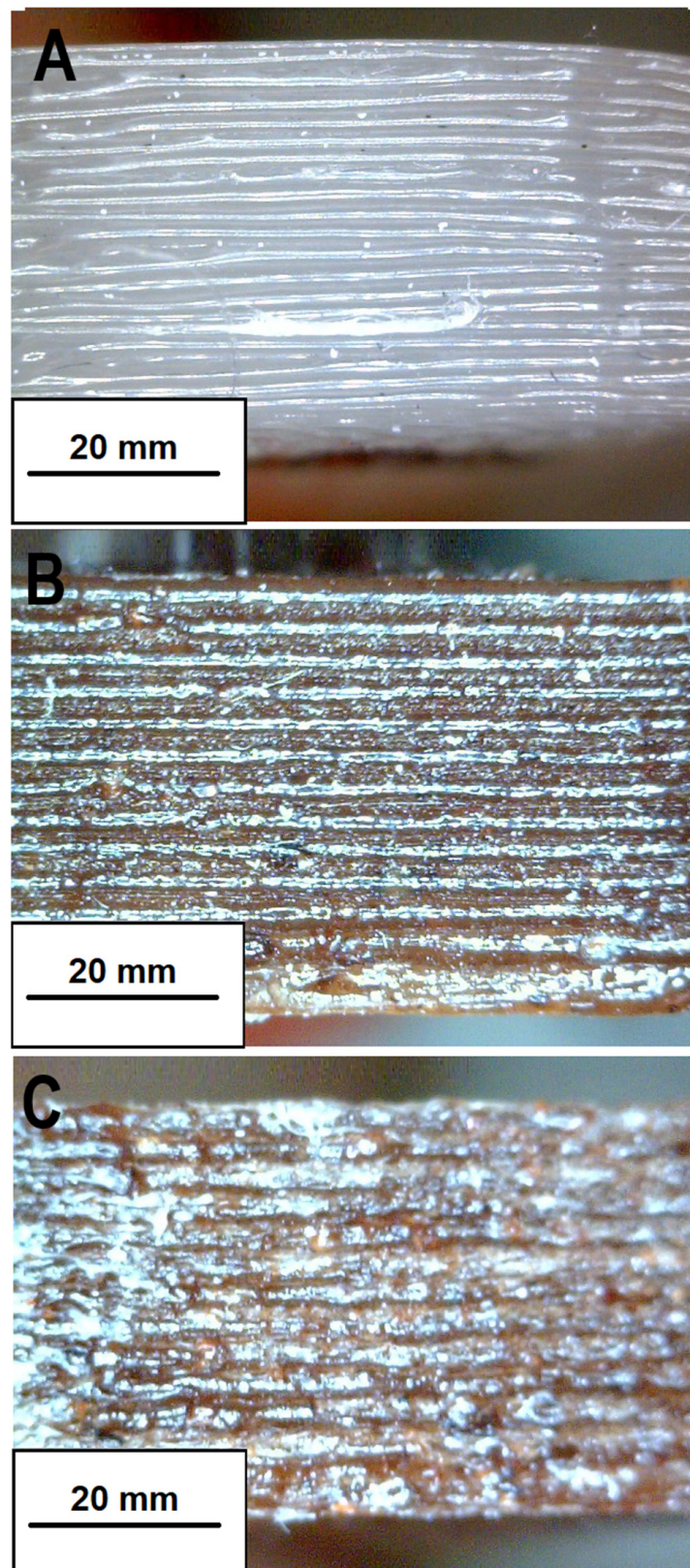


**Figure 9.** Magnified images (50 X) of the 3D bars: (A) printing surface of the 100PLA\_3D specimen; (B) printing surface of the 95PLA/5CBSW\_3D specimen; (C) printing surface of the 90PLA/10CBSW\_3D specimen.



**Figure 10.** Manufactured filament (A), CAD model created with Rhinoceros version 7 software (Robert McNeel & Associates, Seattle, DC, USA) (B) and representative printed samples (C).

#### 4. Conclusions

In this study, novel green composite filaments for FFF were developed and characterized, utilizing cocoa bean shell waste and polylactic acid. Structural–morphological, thermal, and mechanical characterization of both raw materials and products (extruded filaments and 3D printed specimens) was comprehensively conducted. Overall, the findings revealed significant filler aggregates at 10 wt.% CBSW concentration in the PLA matrix. However, at both CBSW concentrations (5 wt.% and 10 wt.%), no notable morphological or thermal alterations were observed, and satisfactory printability was achieved. Moreover, tensile tests on the 3D printed objects demonstrated enhanced rigidity in these specimens and better load resistance at the highest CBSW concentrations. Finally, the biofilament exhibiting superior properties (containing the 10 wt.% of CBSW) was utilized to fabricate some simple 3D printed chocolate models, showcasing the efficacy of the proposed approach in successfully recycling agro-industrial waste within the same production company, leading to economic and ecological benefits. Future research endeavors aim to identify biomarkers confirming the longevity of cocoa organoleptic properties post-printing process and investigate the durability of biocomposites under controlled environmental conditions.

**Author Contributions:** Conceptualization, C.E.C.; software, V.D.C. and D.R.; validation, C.E.C. and D.F.; formal analysis, D.F. and D.R.; data curation, C.E.C., D.F. and D.R.; writing—original draft preparation, C.E.C., D.F. and D.R.; writing—review and editing, C.E.C., D.F. and D.R.; visualization, C.E.C., D.F. and D.R.; supervision, C.E.C., D.F. and D.R. All authors have read and agreed to the published version of the manuscript.

**Funding:** This research was funded by Ministero dell’Istruzione dell’Università e della Ricerca (project PON R&I 2014–2020, D.M. 1061 del 10/8/2021–37° ciclo-Azione IV.5, Dottorati su Tematiche Green, 2021).

**Institutional Review Board Statement:** Not applicable.

**Informed Consent Statement:** Not applicable.

**Data Availability Statement:** Data are contained within the article.

**Acknowledgments:** The authors thank the company “Maglio Arte Dolciaria S.R.L.” (Maglie, Lecce, Italy) for providing the recycled raw material.

**Conflicts of Interest:** The authors declare no conflicts of interest.

#### References

1. Fico, D.; Rizzo, D.; Casciaro, R.; Corcione, C.E. A Review of Polymer-Based Materials for Fused Filament Fabrication (FFF): Focus on Sustainability and Recycled Materials. *Polymers* **2022**, *14*, 465. [\[CrossRef\]](#)
2. Zhang, P.; Wang, Z.; Li, J.; Li, X.; Cheng, L. From materials to devices using fused deposition modeling: A state-of-art review. *Nanotechnol. Rev.* **2020**, *9*, 1594–1609. [\[CrossRef\]](#)
3. Verter, N. Cocoa export performance in the world’s largest producer. *Bulg. J. Agric. Sci.* **2016**, *22*, 713–721.
4. Mendoza-Meneses, C.J.; Feregrino-Pe’rez, A.A.; Gutierrez-Antonio, C. Potential Use of Industrial Cocoa Waste in Biofuel Production. *J. Chem.* **2021**, *2021*, 3388067. [\[CrossRef\]](#)

5. Morettini, G.; Palmieri, M.; Capponi, L.; Landi, L. Comprehensive characterization of mechanical and physical properties of PLA structures printed by FFF-3D-printing process in different directions. *Progr. Addit. Manuf.* **2022**, *7*, 1111–1122. [[CrossRef](#)]
6. Pang, X.; Zhuang, X.; Tang, Z.; Chen, X. Polylactic acid (PLA): Research, development and industrialization. *Biotechnol. J.* **2010**, *5*, 1125–1136. [[CrossRef](#)]
7. Ivanova, O.; Williams, C.; Campbell, T. Additive manufacturing (AM) and nanotechnology: Promises and challenges. *Rapid Prototyp. J.* **2013**, *19*, 353–364. [[CrossRef](#)]
8. González-Henríquez, C.M.; Sarabia-Vallejos, M.A.; Rodríguez-Hernández, J. Polymers for additive manufacturing and 4Dprinting: Materials, methodologies and biomedical applications. *Prog. Polym. Sci.* **2019**, *94*, 57–116. [[CrossRef](#)]
9. Wang, X.; Jiang, M.; Zhou, Z.; Gou, J.; Hui, D. 3D printing of polymer matrix composites: A review and prospective. *Compos. Part B Eng.* **2017**, *110*, 442–458. [[CrossRef](#)]
10. Daminabo, S.C.; Goel, S.; Grammatikos, S.A.; Nezhad, H.Y.; Thakur, V.K. Fused deposition modeling-based additive manufacturing (3D printing): Techniques for polymer material systems. *Mater. Today Chem.* **2020**, *16*, 100248. [[CrossRef](#)]
11. Wu, H.; Fahy, W.P.; Kim, S.; Kim, H.; Zhao, N.; Pilato, L.; Kafi, A.; Bateman, S.; Koo, J.H. Recent developments in polymers/polymer nanocomposites for additive manufacturing. *Prog. Mater. Sci.* **2020**, *111*, 100638. [[CrossRef](#)]
12. Fico, D.; Rizzo, D.; De Carolis, V.; Montagna, F.; Esposito Corcione, C. Sustainable polymer composites manufacturing through 3D printing technologies by using recycled polymer and filler. *Polymers* **2022**, *14*, 3756. [[CrossRef](#)]
13. Khalid, M.Y.; Arif, Z.U. Novel biopolymer-based sustainable composites for food packaging applications: A narrative review. *Food Packag. Shelf Life* **2022**, *33*, 100892. [[CrossRef](#)]
14. Fico, D.; Rizzo, D.; De Carolis, V.; Montagna, F.; Palumbo, E.; Esposito Corcione, C. Development and characterization of sustainable PLA/Olive wood waste composites for rehabilitation applications using Fused Filament Fabrication (FFF). *J. Build. Eng.* **2022**, *56*, 104673. [[CrossRef](#)]
15. Sanyang, M.L.; Sapuan, S.M.; Haron, M. Effect of cocoa pod husk filler loading on tensile properties of cocoa pod husk/polylactic acid green biocomposite films. *AIP Conf. Proc.* **2017**, *1891*, 1.
16. Papadopoulou, E.L.; Paul, U.C.; Tran, T.N.; Suarato, G.; Ceseracchi, L.; Marras, S.; d’Arcy, R.; Athanassiou, A. Sustainable Active Food Packaging from Poly(lactic acid) and Cocoa Bean Shells. *ACS Appl. Mater. Interfaces* **2019**, *11*, 34. [[CrossRef](#)]
17. Tran, T.N.; Bayer, I.S.; Heredia-Guerrero, J.A.; Frugone, M.; Lagomarsino, M.; Maggio, F.; Athanassiou, A. Cocoa Shell Waste Biofilaments for 3D Printing Applications. *Macromol. Mater. Eng.* **2017**, *302*, 1700219. [[CrossRef](#)]
18. Leonard, J.; Berrio, V. *Desarrollo y Caracterización de un Material Compuesto con Fibra de Cacao Para la Producción de Filamento Para Impresión 3D*; Departamento de Ingeniería Química y de Alimentos, Universidad de los Andes: Bogotá, Colombia, 2021.
19. Shanmugam, V.; Pavan, M.V.; Babu, K.; Karnan, B. Fused deposition modeling based polymeric materials and their performance: A review. *Polym. Compos.* **2021**, *42*, 5656–5677. [[CrossRef](#)]
20. Gardan, G. *Additive Manufacturing Technologies in Additive Manufacturing Handbook*; CRC Press: Boca Raton, FL, USA, 2017; p. 20.
21. Garcia-Brand, A.J.; Morales, M.A.; Hozman, A.S.; Ramirez, A.C.; Cruz, L.J.; Maranon, A.; Muñoz-Camargo, C.; Cruz, J.C.; Porras, A. Bioactive Poly(lactic acid)–Cocoa Bean Shell Composites for Biomaterial Formulation: Preparation and Preliminary In Vitro Characterization. *Polymers* **2021**, *13*, 3707. [[CrossRef](#)]
22. Yu, W.; Shi, J.; Qiu, R.; Lei, W. Degradation Behavior of 3D-Printed Residue of Astragalus Particle/Poly(Lactic Acid) Biocomposites under Soil Conditions. *Polymers* **2023**, *15*, 1477. [[CrossRef](#)]
23. De Kergariou, C.; Saidani-Scott, H.; Perriman, A.; Scarpa, F.; Le Duigou, A. The influence of the humidity on the mechanical properties of 3D printed continuous flax fibre reinforced poly(lactic acid) composites. *Compos. Part A Appl. Sci. Manuf.* **2022**, *155*, 106805. [[CrossRef](#)]
24. Depuydt, D.; Balthazar, M.; Hendrickx, K.; Six, W.; Ferraris, E.; Desplentere, F.; Ivens, J.; Van Vuure, A.W. Production and characterization of bamboo and flax fiber reinforced polylactic acid filaments for fused deposition modeling (FDM). *Polym. Compos.* **2019**, *40*, 5. [[CrossRef](#)]
25. Garcia-Brand, A.J.; Maranon, A.; Muñoz-Camargo, C.; Cruz, J.C. Potential Bone Fillers Based on Composites of Cocoa Bean Shells and Poly(Lactic Acid): Compression Molding Manufacturing. In Proceedings of the IEEE 2nd International Congress of Biomedical Engineering and Bioengineering (CI-IB&BI), Bogota D.C., Colombia, 13–15 October 2021.
26. *UNI EN ISO 527-2:2012*; Materie Plastiche—Determinazione Delle Proprietà a Trazione—Parte 2: Condizioni di Prova per Materie Plastiche per Stampaggio ed Estrusione. ISO: Geneva, Switzerland, 2012.
27. Chieng, B.W.; Ibrahim, N.A.; Yunus, W.M.Z.W.; Hussein, M.Z. Poly (lactic acid)/Poly (ethylene glycol) Polymer Nanocomposites: Effects of Graphene Nanoplatelets. *Polymers* **2014**, *6*, 93–104. [[CrossRef](#)]
28. Hoyos, C.G.; Márquez, P.M.; Vélez, L.P.; Guerra, A.S.; Eceiza, A.; Urbina, L.; Vélasquez-Cock, J.; Rojo, P.G.; Acosta, L.V.; Zuluaga, R. Cocoa shell: An industrial by-product for the preparation of suspensions of holocellulose nanofibers and fat. *Cellulose* **2020**, *27*, 10873–10884. [[CrossRef](#)]
29. Lionetto, F.; Del Sole, R.; Cannoletta, D.; Vasapollo, G.; Maffezzoli, A. Monitoring Wood Degradation during Weathering by Cellulose Crystallinity. *Materials* **2012**, *5*, 10. [[CrossRef](#)]
30. Puglia, D.; Dominici, F.; Badalotti, M.; Santulli, C.; Kenny, J.M. Tensile, Thermal and Morphological Characterization of Cocoa Bean Shells (CBS)/Polycaprolactone-Based Composites. *J. Renew. Mater.* **2016**, *4*, 3. [[CrossRef](#)]
31. Le Révérend, B.J.D.; Fryer, P.J.; Coles, S.; Bakalis, S. A Method to Qualify and Quantify the Crystalline State of Cocoa Butter in Industrial Chocolate. *J. Am. Oil Chem. Soc.* **2010**, *87*, 3. [[CrossRef](#)]

32. Reignier, J.; Tatibouët, J.; Gendron, R. Effect of Dissolved Carbon Dioxide on the Glass Transition and Crystallization of Poly (lactic acid) as Probed by Ultrasonic Measurements. *J. Appl. Polym. Sci.* **2009**, *112*, 1345–1355. [[CrossRef](#)]
33. Bryś, A.; Bryś, J.; Ostrowska-Ligeza, E.; Kaleta, A.; Górnicki, K.; Głowacki, S.; Koczoń, P. Wood biomass characterization by DSC or FT-IR spectroscopy. *J. Therm. Anal. Calorim.* **2016**, *126*, 27–35. [[CrossRef](#)]
34. Tsujiyama, S.; Miyamori, A. Assignment of DSC thermograms of wood and its components. *Thermochim. Acta* **2000**, *351*, 177–181. [[CrossRef](#)]
35. Carichino, S.; Scanferla, D.; Fico, D.; Rizzo, D.; Ferrari, F.; Jordá-Reolid, M.; Martínez-García, A.; Esposito Corcione, C. Poly-Lactic Acid-Bagasse Based Bio-Composite for Additive Manufacturing. *Polymers* **2023**, *15*, 4323. [[CrossRef](#)] [[PubMed](#)]
36. De Armitt, C.; Hancock, M. Filled Thermoplastics. In *Particulate-Filled Polymer Composites*, 2nd ed.; Rothon, R.N., Ed.; Rapra Technology Limited: Shrewsbury, UK, 2003.

**Disclaimer/Publisher’s Note:** The statements, opinions and data contained in all publications are solely those of the individual author(s) and contributor(s) and not of MDPI and/or the editor(s). MDPI and/or the editor(s) disclaim responsibility for any injury to people or property resulting from any ideas, methods, instructions or products referred to in the content.